CHEMICAL ENGINEERING TRANSACTIONS
VOL. 62, 2017
A publication of AIDIC
The Italian Association of Chemical Engineering
Online at www.aidic.it/cet
Guest Editors: Fei Song, Haibo Wang, Fang He

**ISBN** 978-88-95608- 60-0; **ISSN** 2283-9216
DOI: 10.3303/CET1762171

# Effects of Different Fly Ash Proportion on the Physical and Mechanical Performance and Pore Structure of Foam Concrete

Chengyun Tao[a], Shuhui Dong[b]

[a]Harbin University, Heilongjiang Provincial Key Laboratory of Underground Engineering Technology, Harbin 150086, China
[b]Harbin Institute of Technology, Harbin 150001, China
gxtaocy@hrbu.edu.cn

In order to make better use of industrial solid waste fly ash to develop new foam concrete building materials, the different fly ash proportions are studied and dry density, mechanical performance and appearance of microstructure of foam cement with different ages are analyzed in this paper. The results show that the proportion of fly ash makes the performance of foam concrete develop in the adverse direction, and the proportion of fly ash should be strictly controlled. When the amount of fly ash replacing cement is 900g (i.e., fly ash accounts for 22.5 % of aggregate), the performance of the test block is more appropriate and in the best "cost performance" state. Under this condition, the dry apparent density of foam cement is 456 kg/m3 at 28 days of age, and the compressive strength is 2.34 MPa.

## 1. Introduction

Foam concrete insulation block is a kind of insulation wall masonry material made of cement as the main cementing material through the chemical foaming process, with the characteristics of light weight, good thermal insulation, fire resistance, durability, low cost and making full use of building waste (Ayrikyan et al., 2017). It is a composite lightweight material formed by uniform mixing, moulding and hardening, de-moulding and maintenance through in-situ foaming after the foaming agent is added into the cement-based slurry after mixing (Chen et al., 2015). The dry apparent density of foam concrete is relatively small. The dry density of common foam concrete is 300-1200 kg/m3; the consistency of slurry can be controlled which is convenient for construction and the strength is controlled (Choi and Popovics, 2015). Since a large amount of industrial waste, such as fly ash, can be incorporated into foam concrete to serve as its filled aggregate, it is quite beneficial and of great significance to study this new material for protecting the environment and gradually diminished land resources (Cipriani et al., 2016). And the prospect is quite excellent (Deller et al., 2015).
Building waste for the production of foam concrete blocks opens up a new way for recycling of construction waste (Dittrich et al., 2013). Waste concrete and waste sintered brick are the main components of construction waste. Studies have shown that the quality stability of recycled raw material of foam concrete can be effectively controlled by optimizing the mix design and adding the active mixture (Dorotovič et al., 2014). Fly ash has morphological effect, micro-aggregate effect and active effect (Guo et al., 2016), which is one of the most commonly used active mixes. This paper mainly studies the strengthening effect of fly ash on recycled foam concrete under the condition of natural curing (Henriques, 2012).

## 2. Raw materials and test methods

### 2.1 Raw materials

The raw materials in the experiment include fly ash, sand, cement, polypropylene fiber, gypsum, water reducer, foaming agent, foam stabilizer, thickener and others, of which there are the first-grade fly ash produced by a power plant, ordinary sand filtered with a standard sieve of 0.9 mm, ordinary portland cement of Grade 42.5 produced by Henan Jiaozuo Cement Co., Ltd., water reducer commercially available as Dechang brand with

Please cite this article as: Chengyun Tao, Shuhui Dong, 2017, Effects of different fly ash proportion on the physical and mechanical performance and pore structure of foam concrete, Chemical Engineering Transactions, 62, 1021-1026 DOI:10.3303/CET1762171

the main component of polyhydroxy acid (Hovden et al., 2014) and self-made hydrogen peroxide foaming agent.

### 2.2 Experimental Methods

The comparative experiment is conducted according to the different ratio in Table 1. Firstly, weigh the fly ash, cement, sand, foam stabilizer, thickener (Huang et al., 2014), water reducer and other materials with an electronic scale and add them to a small bucket at the same time and stir them well with a gray shovel (Ivankina and Matthies, 2015); then use a measuring cup to weigh amount of water with the temperature of 20 ℃ and slowly pour into the keg; stir the slurry in the keg with a homemade blender with the speed of about 20 rev/s; observe the consistency of the slurry (Kondrashova et al., 2013); add appropriate amount of water reducing agent if it is too thick until it has good fluidity in order to better mold (Lam and Esfeld, 2013); and finally weigh appropriate amount of foaming agent with electronic scales; quickly pour it into the slurry solution and stir for 5 seconds with a homemade stirrer (Liszkay et al., 2013) to rapidly spread the foaming agent, and then life the keg and pour the foam concrete pulp into the abrasive tool of plastic bucket, and observe the foaming phenomenon(Ma, et al., 2016). During this process, the actual proportion of various materials during the experiment is recorded (Maslov, 2016). After hardening of the slurry molded (about 12 hours), appropriate amount of water is added in the mold for curing and thus make the added water overflow about 20 mm from the test block (Ming et al., 2013).

*Table 1: The mix proportion experiment of fiber foam concrete*

| Number | Fly ash (g) | Cement (g) | Water (g) | Sand (g) | Gypsum (g) | Blowing agent (g) | Water reducing agent (g) |
|---|---|---|---|---|---|---|---|
| 1 | 500 | 2000 | 1250 | 900 | 600 | 130 | 8 |
| 2 | 900 | 1600 | 1250 | 900 | 600 | 130 | 8.5 |
| 3 | 1300 | 1200 | 1250 | 900 | 600 | 135 | 10 |
| 4 | 1700 | 800 | 1250 | 900 | 600 | 140 | 10.5 |

## 3. Experimental results and analysis

It is found in this experiment that there are great changes in the performance after the proportion is changed. After the experiment we measured the dry density, compressive strength, splitting tensile strength and other physical quantities of foam concrete after 7d, 14d and 28d. The detailed experimental results are shown in Table 2. During the experiment, when the fly ash proportion is 1300g, the slurry hardens quickly. After moulding, it is very difficult for the foaming agent to foam the slurry. The reason may be that the slurry hardens quickly after the addition of gypsum and fly ash, (Qiao et al, 2012), and finally the bubbles overflow from the middle, resulting in that the test blocks do not reach the desired height. Therefore, the amount of water reducer and foaming agent is increased appropriately (Qiao et al, 2013). When the fly ash proportion is 500g, cracks appear on the surface of test block after moulding for about 30 minutes.

*Table 2: The influence of foamed concrete performance by different fly ash content*

| Days | Number | Dry density (kg/m³) | Compressive strength (MPa) | Tensile strength (MPa) |
|---|---|---|---|---|
| 7 | 1 | 418 | 0.79 | 0.35 |
| | 2 | 453 | 0.65 | 0.31 |
| | 3 | 460 | 0.54 | 0.24 |
| | 4 | 467 | 0.51 | 0.19 |
| 14 | 1 | 425 | 1.89 | 0.67 |
| | 2 | 455 | 1.65 | 0.61 |
| | 3 | 461 | 1.56 | 0.59 |
| | 4 | 470 | 1.31 | 0.52 |
| 28 | 1 | 430 | 2.56 | 1.34 |
| | 2 | 456 | 2.34 | 1.12 |
| | 3 | 460 | 2.12 | 1.0 |
| | 4 | 478 | 1.89 | 0.89 |

### 3.1 Influence of fly ash proportion on dry density and pore structure of foam concrete

It can be seen from Figure 1 that as the amount of fly ash instead of cement increases, the density of foam concrete (dry apparent density) gradually increases. They are almost in a linear scale relationship. The amount of fly ash instead of cement is increased from 500g to 1700g. The dry apparent density is increased from 418 kg/m3 to 467 kg/m3 at 7d of the foam concrete test block; the increase rate is 11.72%. The dry apparent density at 14d is increased from 425 kg/m3 to 470 kg/m3, and the decrease rate is 10.59%. The dry apparent density is increased from 430 kg/m3 to 478 kg/m3 at 28d, and the increase rate is 11.16%. Therefore, the increase rate of dry apparent density is increased with the increase of age, and its change is not obvious (Schussler, 2013). At the same time, it can be seen from Figure 1 that: the dry apparent density at 7d, 14d and 28d is relatively close, that is, dry apparent density is not closely related to the age (Sobotka et al., 2013). It can be seen that fly ash proportion has the obvious effects on the density of foam concrete.

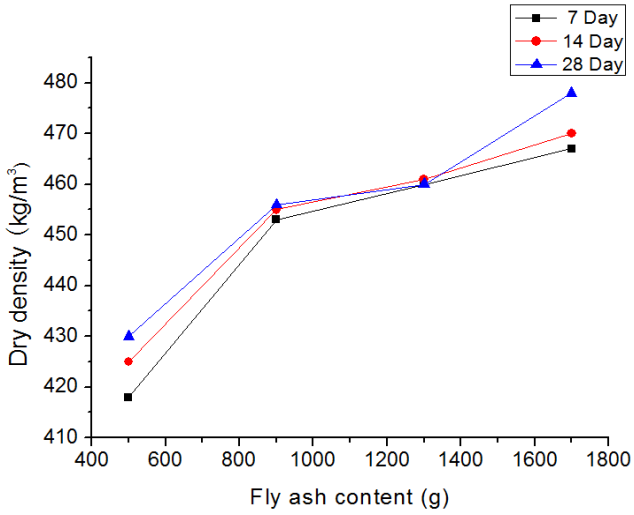


*Figure 1: The influence of foamed concrete for dry density by different fly ash content*

As the fly ash with different proportions is used instead of cement in this experiment, there are impurities in the fly ash. The partial fly ash will be in hydration reaction (Thiemann and Zipfel, 2014). Therefore, the free moisture will increase. The greater the fly ash proportion is, the greater the porosity of the foam concrete is, and the greater the final density is (Ushizima, et al, 2012). The pore structure with the change of fly ash proportion is shown in Figure 2.

### 3.2 Influence of fly ash proportion on mechanical properties of foam concrete

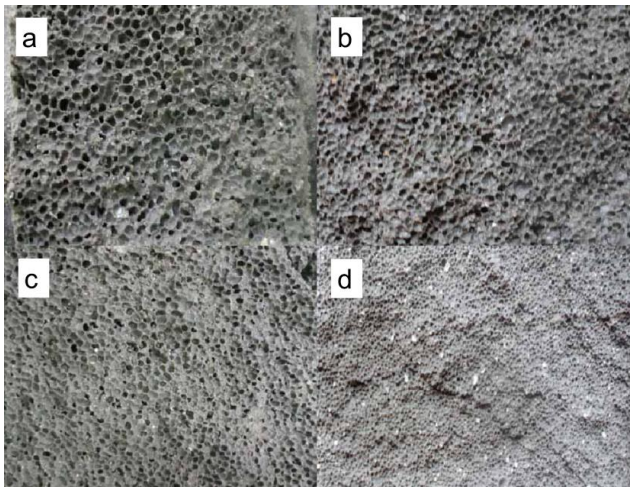


*Figure 2: The influence of foamed concrete for pore structure by different fly ash content (a) Fly ash 500g (b) Fly ash 900g (c) Fly ash 1300g (d) Fly ash 1700g*

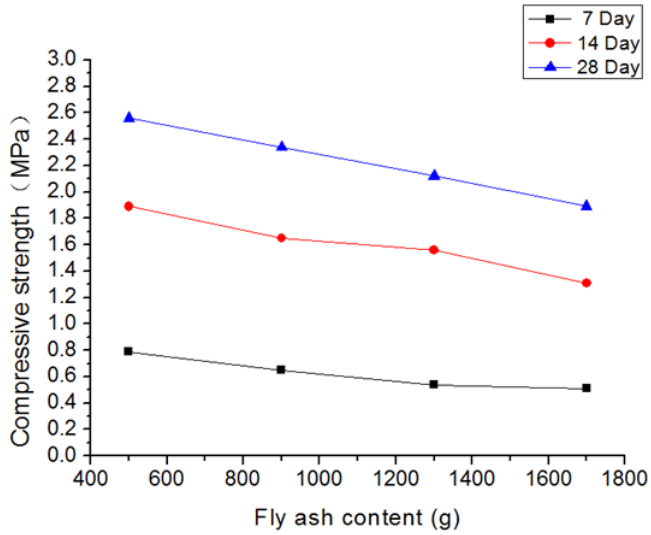


*Figure 3: The influence of foamed concrete for compressive strength by different fly ash content*

From Figure 2 and 3, it can be seen that with the increase of the amount of fly ash instead of cement, the compressive strength and splitting tensile strength tend to decrease greatly (Wang et al, 2016). The amount of fly ash replacing cement is increased from 500g to 1700g; the compressive strength of the test block at 7d is decreased from 0.79MPa to 0.51MPa, and the reduction rate is 35.44%; the compressive strength of the test block at 14d is decreased from 1.89MPa to 1.31MPa, and the reduction rate is 30.69%. The compressive strength at 28d is decreased from 2.56MPa to 1.89MPa, and the reduction rate is 26.17%. At the same time, it can be seen from Figure 4-21 that the splitting tensile strength at 7d is decreased from 0.35MPa to 0.19MPa, and the reduction rate is 45.71%; the splitting tensile strength at 14d is decreased from 0.67MPa to 0.52MPa, and the reduction rate is 22.39%. The splitting tensile strength at 28d is decreased from 1.34MPa to 0.89MPa, and the reduction rate is 33.58%. With the increase of age, the decrease rate of splitting tensile strength of the test block decreases first and then increases.

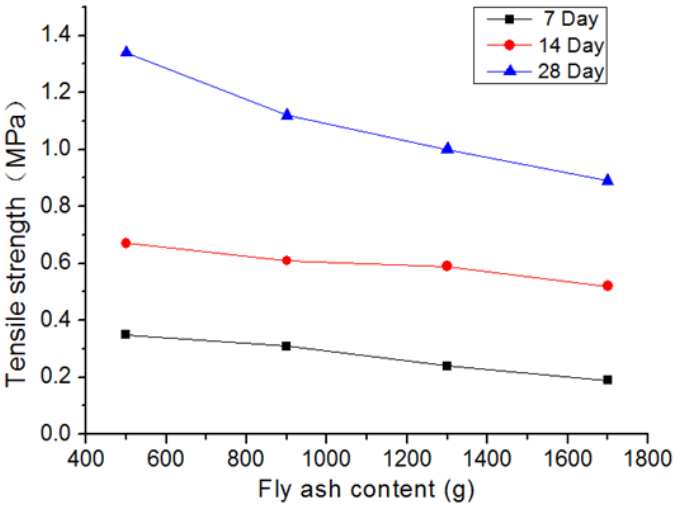


*Figure 4: The influence of foamed concrete for tensile strength by different fly ash content*

In summary, the effect of fly ash content on the compressive strength and splitting tensile strength of foam concrete is significant. As the age increases, that is, the age increases from 7 to 28 days and the fly ash content is 500g, the compressive strength increases from 0.79MPa to 2.56MPa; when the fly ash content is 900g, the compressive strength increases from 0.65MPa to 2.34MPa; when the fly ash content is 1300g, the compressive strength increases from 0.54MPa to 2.12MPa; when the fly ash content is 1700g, the

compressive strength increases from 0.51MPa to 1.89MPa. When the fly ash content is 500g, the splitting tensile strength increases from 0.35MPa to 1.34MPa; when the fly ash content is 900g, the splitting tensile strength increases from 0.31MPa to 1.12MPa; When the fly ash content is 1300g, the splitting tensile strength increases from 0.24MPa to 1.0MPa; when the fly ash content is 1700g, the splitting tensile strength increases from 0.19MPa to 0.89MPa; It can be seen that the compressive strength and splitting tensile strength of foam concrete increase with the increase of age, and the impact is also significant.

## 4. Conclusion

In this paper, the influence of single factor in each experiment on the physical properties, mechanical properties and pore structure of the foam concrete test block is analyzed through three groups of comparative experiments according to the experimental method of changing single factor. Finally, the following conclusions are drawn: As the amount of ash replacing cement increases, the consistency of foam concrete slurry varies greatly, and the amount of water reducer must be increased significantly, which indicates that the hydration reaction of fly ash requires more water than cement; with the increase of fly ash, dry apparent density increases, but the intensity decreases, which indicates that there are more impurities in fly ash or the fly ash is not activated. The addition of fly ash makes the bubble distribute non-uniformly, so that it is necessary to strict control the fly ash proportion. Through the research and analysis in the experiment, it can be seen that when the amount of fly ash instead of cement is 900g (i.e., fly ash accounts for 22.5 % of aggregate), the performance of the test block is more appropriate; the dry apparent density is 456 kg/m3 at 28 days, and the compressive strength is 2.34 MPa. Under this condition, the foam concrete test block is of better “cost performance”.

### Reference


Ayrikyan A., Kastner A., Khansur N. H., Yasui S., Itoh M., Webber K. G., 2017, Lead-Free Multilayer Piezoceramic Composites: Effect of Cosintering on Electromechanical Properties, and Frequency Control IEEE Transactions on Ultrasonics, Ferroelectrics, 64, 1127-1134, DOI: 10.1109/TUFFC.2017.2701882

Chen X., Pang J., Zhou G., 2015, Simple route to prepare different core --shell structured silica-based microspheres, IET Micro Nano Letters, 10, 310-314, DOI: 10.1049/mnl.2015.0035

Choi H., Popovics J.S., 2015, NDE application of ultrasonic tomography to a full-scale concrete structure, and Frequency Control IEEE Transactions on Ultrasonics, Ferroelectrics, 62, 1076-1085, DOI: 10.1109/TUFFC.2014.006962

Cipriani M., Gus'kov S.Y., Angelis R.D., Andreoli P., Consoli F., Cristofari G., Giorgio G.D., Ingenito F., Rupasov A.A., 2016, Powerful laser pulse absorption in partly homogenized foam plasma, JINST, 11, C03062, DOI: 10.1088/1748-0221/11/03/C03062

Deller A., Cooper B.S., Wall T.E., Cassidy D.B., 2015, Positronium emission from mesoporous silica studied by laser-enhanced time-of-flight spectroscopy, New J. Phys., 17, 043059, DOI: 10.1088/1367-2630/17/4/043059

Dittrich B., Hellmann F., Kaminski W., 2013, Holonomy Spin Foam Models: Boundary Hilbert spaces and Time Evolution Operators, Class. Quant. Grav., 30, 085005, DOI: 10.1088/0264-9381/30/8/085005

Dorotovič I., Erdélyi R., Freij N., Karlovský V., Márquez I., 2014, Standing sausage waves in photospheric magnetic waveguides, Astron, Astrophys., 563, A12, DOI: 10.1051/0004-6361/201220542

Guo B., Huang Y., Gong Q., Wang J., Zhuang D., Liang J., 2016, Flexible route to fabricate excellent adsorbents for vitamin B12 by specially designed oil-drop process, IET Micro Nano Letters, 11, 188-191, DOI: 10.1049/mnl.2015.0491

Henriques V.M.J., 2012, 3D Temperature Mapping of Solar Photospheric Fine Structure Using Ca II H Filtergrams, Astron, Astrophys., 548, A114, DOI: 10.1051/0004-6361/201220344

Hovden R., Ercius P., Jiang Y., Wang D., Yu Y., Abruna H.D., Elser V., Muller D.A., 2014, Breaking the Crowther Limit: Combining Depth-Sectioning and Tilt Tomography for High-Resolution, Wide-Field 3D Reconstructions, Ultramicroscopy, 140, 26-31, DOI: 10.1016/j.ultramic.2014.01.013

Huang Q., Cai X., Alhadj-Mallah M.M., Du C., Chi Y., Yan J., 2014, Thermal Plasma Vitrification of MSWI Fly Ash Mixed With Different Biomass Ashes, IEEE Transactions on Plasma Science, 42, 3549-3554, DOI: 10.1109/TPS.2014.2358626

Ivankina T.I., Matthies S., 2015, On the development of the quantitative texture analysis and its application in solving problems of the Earth sciences, Phys. Part. Nucl, 46, 366-423, DOI: 10.1134/S1063779615030077

Kondrashova N.N., Pasechnik M.N., Chornogor S.N., Khomenko E.V., 2013, Atmosphere dynamics of the active region NOAA 11024, Solar Phys., 284, 499, DOI: 10.1007/s11207-012-0212-5

Lam V., Esfeld M., 2013, A dilemma for the emergence of spacetime in canonical quantum gravity, Stud. Hist. Phil. Sci., B44, 286-293, DOI: 10.1016/j.shpsb.2012.03.003

Liszkay L., Comini P., Corbel C., Debu P., Dupré P., Grandemange P., Pérez P., Rey J.M., Ruiz N., Sacquin Y., 2013, Linac-based positron source and generation of a high density positronium cloud for the GBAR experiment, J. Phys. Conf. Ser., 443, 012006, DOI: 10.1088/1742-6596/443/1/012006

Ma Y.W., Oh J.Y., Ahn S., Shin B.S., 2016, A method for fabricating a micro-structured surface of polyimide with open and closed pores, J. Korean Phys. Soc., 69, 386-389, DOI: 10.3938/jkps.69.386

Maslov O.D., 2016, Results of high temperature processing of high-carbon materials from the lower Cambrian period of the Earth's history, Phys. Part. Nucl. Lett, 13, 521-525, DOI: 10.1134/S1547477116040087

Ming R., Ding Y., Chang F., He X., Feng J., Wang C., Zhang P., 2013, Humidity-dependant compression properties of graphene oxide foams prepared by freeze-drying technique, IET Micro Nano Letters, 8, 66-67, DOI: 10.1049/mnl.2012.0833

Qiao G., Hong Y., Song G., 2012, Potential Sensor Based on Electrochemical rm NiFe_2rm O_4 Film Prepared by EB-PVD, IEEE Sensors Journal, 12, 2664-2665, DOI: 10.1109/JSEN.2012.2200100

Qiao G., Hong Y., Sun G., Yang O., 2013, Corrosion Energy: A Novel Source to Power the Wireless Sensor, IEEE Sensors Journal, 13, 1141-1142, DOI: 10.1109/JSEN.2012.2227596

Schussler M., 2013, Solar magneto-convection, IAU Symp., 294, 95-106, DOI: 10.1017/S1743921313002329

Sobotka M., Svanda M., Jurcak J., Heinzel P., Del M.D., Berrilli F., 2013, Dynamics of the solar atmosphere above a pore with a light bridge, Astron, Astrophys., 560, A84, DOI: 10.1051/0004-6361/201322148

Thiemann T., Zipfel A., 2014, Linking covariant and canonical LQG II: Spin foam projector, Class. Quant, Grav, 31, 125008, DOI: 10.1088/0264-9381/31/12/125008

Ushizima D., Morozov D., Weber G.H., Bianchi A.G.C., Sethian J.A., Bethel E.W., 2012, Augmented Topological Descriptors of Pore Networks for Material Science, IEEE Transactions on Visualization and Computer Graphics, 18, 2041-2050, DOI: 10.1109/TVCG.2012.200

Wang H., Guo H., Liu Y., Yi C., Chu J., 2016, Regeneration of Activated Carbon Spent with Phenol and Formation of Hydrogen Peroxide in a Pulsed Discharge Plasma System, IEEE Transactions on Plasma Science, 44, 1834-1841, DOI: 10.1109/TPS.2016.2593708